Free Surface Profile and Surface Tension in a Polymer Melt: A Monte Carlo Study

P. Cifra,† E. Nies,‡ and F. E. Karasz*,§

Polymer Institute, Slovak Academy of Sciences, 842 36 Bratislava, Slovakia, Department of Polymer Technology, Eindhoven University of Technology, 5600 MB Eindhoven, The Netherlands, and Department of Polymer Science and Engineering, University of Massachusetts, Amherst, Massachusetts 01003

Received May 18, 1993; Revised Manuscript Received November 30, 1993®

ABSTRACT: Monte Carlo (MC) lattice simulation studies have been performed for a compressible polymer melt over a wide range of cohesion energies or densities. The free surface of the melt was examined with respect to its concentration profile, surface thickness D, and surface tension σ. For various reduced intersegmental energies, e ($e < 0$), we found that σ is proportional to $-e^{1/2}$ and that D varies linearly with $(e_c - e)^{-1/2}$, where e_c is a critical value of the reduced intersegmental energy; both relations are analogous to those for a polymer–polymer interface. The surface thickness for a representative system was calculated to be in the range $D \approx 1.5$–4.0 nm. Relative to the values found with the equation-of-state theory for surface tension of Sanchez and Poser and with the functional integral approach of Hong and Noolandi, we observed somewhat lower densities and thicker interfaces for given cohesion energies. The observed surface profiles are also symmetric rather than asymmetric as predicted by these theories. Our equation for the dimensionless parameter σ_{red} versus T_{red} provides realistic values for the surface tension and its temperature coefficient using parameters obtained from data for the bulk polymers. The microscopic analysis of the interface from the MC simulation results revealed a surface enrichment by chain ends, a layering of coil centers beneath the surface, a continuous variation in intersegmental contacts, and a strong deformation of coils in the interface. We also found a slight variation of coil dimensions in the bulk for different temperatures and cohesion energies.

Introduction

The nature of a free polymer surface and of a polymer–polymer interface plays an important role in many applications involving adhesion, friction, wettability, and coating. The effort to understand and control processes involving these applications would benefit from a better understanding of events at the molecular level.[1]

There are few simulation studies of the free surface of a polymer melt;[2-4a] and few such studies have considered compressible systems of variable volume.[5,6] In this contribution we report simulations of a compressible polymer melt with a free surface that result in the determination of the surface tension and the surface thickness from the calculated surface profiles. In these simulations, the variation in these quantities was correlated with changes in cohesion energy, temperature, and density. Attention was also paid to the microstructure of the surface region in terms of segment–segment or segment–void contacts and of the densities of chain ends and coil centers of mass across the surface profile of the melt.

At the molecular level,[7] a polymer–polymer (P/P) interface is understood in greater detail than is a free surface, partially because only the composition varies across the interface whereas a free surface also involves a density variation, a feature that complicates analysis. We have performed MC simulations of the free surface and, for the phenomenological interpretation of the data, have used results derived for the P/P interface in the strong segregation (immiscible) limit,[7-9] an appropriate approximation. In addition, we have compared the present simulation results for surface profiles and surface tension to equation-of-state theory (EOS) predictions.[10,11]

MC Simulations

For MC simulations of low molecular weight liquids, the surface tension σ can be found by using the standard relation[12]

$$\sigma L^2 = \langle \sum_{i<j} \sum (\mathbf{r}_{ij} - 3z_{ij}^2/\mathbf{r}_{ij})\mathbf{u}'(\mathbf{r}_{ij}) \rangle \qquad (1)$$

where $\mathbf{r}_{ij}$ is the distance between molecules, z_{ij} is its z component, $\mathbf{u}'(\mathbf{r}_{ij})$ is the gradient of the potential energy between the molecules, and the summation is taken over all pairs of molecules in the sample area L^2. In the bulk, the term $3z_{ij}^2/\mathbf{r}_{ij}$ averages out to $\mathbf{r}_{ij}$, so the total contribution to σ arises only from pairs of molecules near the interface. On a cubic lattice, we can analyze separately the contributions from the x and y directions (parallel to the surface) and the z direction (perpendicular to the surface). In the x and y directions, after averaging, all contributions in the summation cancel out, because the density gradient is in the z direction. Thus, only the latter is relevant and leads to the term $-2z_{ij}\mathbf{u}'(z_{ij})$ in the double summation in eq 1. In reformulating the continuum approach to that of a lattice with nearest-neighbor interactions and a lattice spacing equal to unity we approximate the gradient $\mathbf{u}'(\mathbf{r}_{ij})$ by $\mathbf{u}'(\mathbf{r}_{ij}) = -\epsilon$.

By using this approximation and the equilibrium densities of segments over the entire surface profile derived from MC lattice simulations of nearest-neighbor interactions, we can sum over the layers of the surface profile rather than over individual molecules and obtain

$$\sigma a^2 = 2\epsilon \sum_z \phi(z)[\phi(z+1) - \phi(z-1)] \qquad (2)$$

where $\phi(z)$ is the equilibrium volume fraction of occupied sites at the respective z coordinate of the profile obtained from the MC simulation, ϵ ($\epsilon < 0$) is the nearest-neighbor

† Slovak Academy of Sciences. Present address: Department of Polymer Technology, Eindhoven University of Technology, 5600 MB Eindhoven, The Netherlands.
‡ Eindhoven University of Technology.
§ University of Massachusetts.
® Abstract published in *Advance ACS Abstracts*, February 1, 1994.

0024-9297/94/2227-1166$04.50/0 © 1994 American Chemical Society

segment–segment cohesive interaction energy, and a is the length of one side of a lattice site. In the simplified case of a steplike profile in which the reduced concentration drops at some given value of z from 1 to 0, only one term in the summation remains finite, and eqs 1 and 2 reduce to $\sigma a^2 = -2\epsilon$, as required.

A natural extension of eq 2 for the free surface of a *miscible* polymer blend containing homopolymers of type A and B yields

$$\sigma_{AB}a^2 = 2\sum_z \{\phi_A(z)[\epsilon_{AA}(\phi_A(z+1) - \phi_A(z-1)) + \epsilon_{AB}(\phi_B(z+1) - \phi_B(z-1))] + \phi_B(z)[\epsilon_{BB}(\phi_B(z+1) - \phi_B(z-1)) + \epsilon_{AB}(\phi_A(z+1) - \phi_A(z-1))]\} \quad (3)$$

where ϵ_{ij} denotes the several nearest-neighbor i,j segment–segment interaction energies and ϕ_i denotes the respective volume fractions.

However, for the A/B interface, an internal surface, exhibiting a continuous change in concentration from polymer A to polymer B, increasing z produces the different result shown below, where the difference is only in the sign of the second term:

$$\sigma_{AB}a^2 = 2\sum_z \{\phi_A(z)[\epsilon_{AA}(\phi_A(z+1) - \phi_A(z-1)) + \epsilon_{AB}(\phi_B(z+1) - \phi_B(z-1))] - \phi_B(z)[\epsilon_{BB}(\phi_B(z+1) - \phi_B(z-1)) + \epsilon_{AB}(\phi_A(z+1) - \phi_A(z-1))]\} \quad (4)$$

From eq 4, for a steplike surface profile (i.e., with a discontinuity from A to B at a given z), as with eq 2, we obtain $\sigma_{AB}a^2 = 2(-\epsilon_{AA} - \epsilon_{BB} + 2\epsilon_{AB})$, as required. Note that further simplification to consider the A homopolymer alone yields the result $\sigma_A a^2 = -2\epsilon_A$, as was obtained from eq 2.

For low molecular weight liquids, eqs 2–4 are formally correct. For polymer chains, however, we need to introduce the multiplication factor $(Z-2)/Z$ in all three equations, which effectively takes only nonbonded contacts into account. Hence, instead of eq 2, we obtain

$$\sigma a^2 = 2\epsilon[(Z-2)/Z]\sum_z \phi(z)[\phi(z+1) - \phi(z-1)] \quad (5)$$

where Z is the appropriate lattice coordination number. This, however, is essentially a combination of a mean-field (MF) and MC approach. A preferred way to calculate σ from a lattice simulation is by using the relation

$$\sigma L^2 = 2\epsilon\langle\sum_i [N_{nb}(z_i,z_i+1) - N_{nb}(z_i,z_i-1)]\rangle \quad (6)$$

which is a restatement of eq 1 for the polymer liquid on the lattice and which accounts properly for nonbonded contacts. The summation in eq 6 is performed over each chain segment i within the three-dimensional surface region (area L^2) and averaging is performed over the many different multichain configurations, as in eq 1. $N_{nb}(z_i,z_i+1)$ and $N_{nb}(z_i,z_i-1)$ are the number of nonbonded contacts of segment i at z_i with sites $z_i + 1$ and $z_i - 1$ respectively. The difference in the number of nonbonded contacts, N_{nb}, for a given segment in opposite directions along the z axis perpendicular to the surface takes the possible values -1, 0, 1. Equation 6 will be used here for the analysis of surface tension; however, as will be shown, eq 5 is in fact a very good approximation.

Mansfield et al.[2] recently proposed another method to calculate σ from molecular simulations by applying an infinitesimal affine deformation of the surface area while keeping the total volume constant.

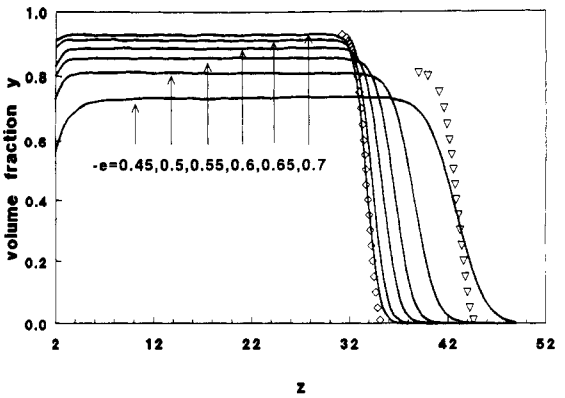

Figure 1. Profiles of occupied volume fraction y as a function of distance z from the wall for various cohesion energies in a polymer melt. Points are the result of the Poser–Sanchez (SP) theory for $e = -0.45$ (▽) and -0.7 (◇).

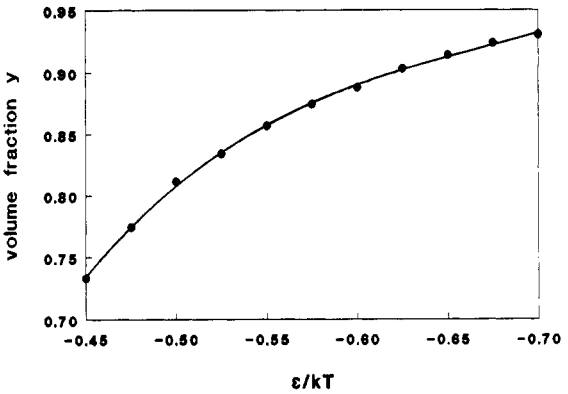

Figure 2. Occupied volume fraction as a function of reduced cohesion energy in the bulk regime.

The MC simulation method used in this analysis has been described in a previous communication.[4a] The polymer melt is simulated by chain conformations on a cubic lattice with nearest-neighbor interaction energy ϵ (here used as a reduced cohesion energy, $e = \epsilon/kT$) between polymer segments. A short-range interaction in the vicinity of a hard wall combined with the imposed cohesion in the melt causes the system of chains to condense against the wall, thereby forming a polymer slab with three distinguishable regions: (i) a region close to the wall–polymer interface, (ii) the bulk, and (iii) the free surface. In this contribution, we report on investigations of the free surface of the melt lying parallel to the wall. A chain length of $N = 30$ segments per chain has been used; other details of the simulation procedure have been described previously.[4a] Because there is no restriction on the exchange of voids between the condensed phase and the external volume, except for that arising from the cohesion in the melt, the system is effectively at zero pressure.[13]

Results and Discussion

Surface Profiles, Surface Tension, and Surface Thickness. Figure 1 depicts profiles of the occupied volume fraction in the polymer melt at equilibrium as a function of distance from the wall (located at $z = 1$) for various cohesion energies in the range $-e = 0.45$–0.7.

The flat region in each profile depicted in Figure 1 provides the density of the bulk polymer phase expressed in terms of an occupied volume fraction y as a function of e; these values are plotted in Figure 2. It is observed that for lower cohesion energies, there are large variations of density with e, whereas at higher energies, an additional increase in cohesion does not bring a proportional increase of density because of a space-filling limitation. These MC

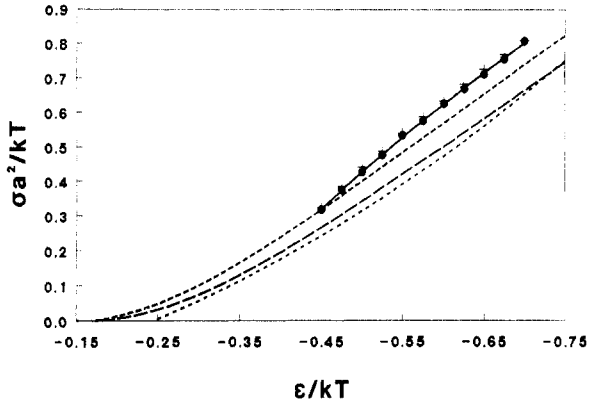

Figure 3. Surface tension $\sigma a^2/kT$ as a function of cohesion energy ϵ/kT: (●) results of eq 6; (+) results of eq 5; (- - -) SP theory results for $N = 30$; (— — and – – –) results of the SP and Hong–Noolandi (HN) theories, respectively, for $N \rightarrow \infty$.

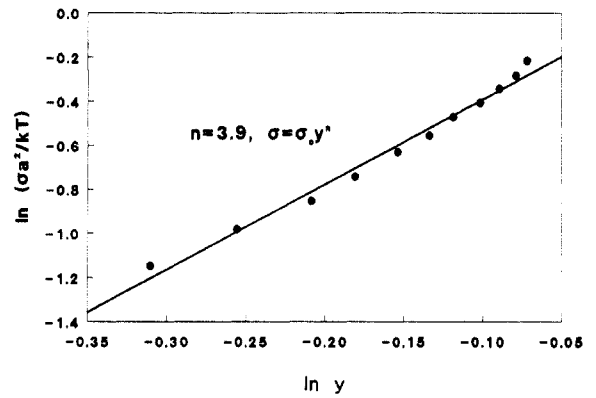

Figure 4. $\ln(\sigma a^2/kT)$ as a function of $\ln y$ for the values used in Figure 3.

results coincide with the liquid branch of the coexistence curve.

In the discussion below, we will concentrate on the free surface region of the profiles.

Figure 3 represents the results of an analysis of the free surface according to the approximation, eq 5, and the more exact MC analysis, eq 6. We find good agreement between the two results. For internal consistency we will nevertheless limit ourselves to results based on eq 6. By extrapolation, we find that the surface tension drops to zero at a critical cohesion energy e_c, which in fact appears to be close to that predicted by the EOS analysis, i.e., $e_c = -0.311$, which incorporates nonrandom mixing and connectivity effects in the analytical theory.[13]

By combining the results of Figures 2 and 3, it would be possible to plot $\sigma a^2/kT$ as a function of volume fraction y. Such a plot would reveal that the surface tension increases with the density and that this increase is steeper for higher densities. However, it is instructive to show this relation (Figure 4) in the form of the empirical plot $\sigma = \sigma_0 y^n$ (known as McLeod's equation[1]), where the exponent n for polymers usually lies between 3 and 4.4. We find some deviation from this relation, but the approximate exponent for our range of densities is found to be $n \sim 3.9$.

A further analysis of σ as a function of e shows that there is a linear relation between $\sigma a^2/kT$ and $-e^{1/2}$ (Figure 5). This can be explained by analogy with a similar relation,[9-11] $\sigma a^2/kT = (\chi/6)^{1/2}$, derived for the interface between two polymers in the strong segregation limit. Thus from $\chi = (Z-2)[\epsilon_{AB} - (\epsilon_{AA} + \epsilon_{BB})/2]$ and $\epsilon_{AB} = \epsilon_{BB} = 0$ (in this simulation), we find that χ is proportional to $-\epsilon_{AA}$, which here is identical to the cohesion energy $-\epsilon$.

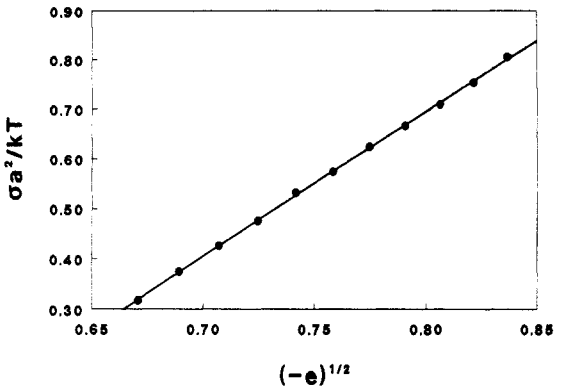

Figure 5. Surface tension $\sigma a^2/kT$ as a function of $-e^{1/2}$ for the values used in Figure 3.

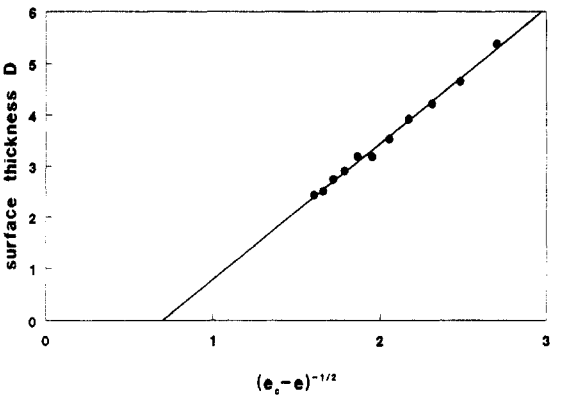

Figure 6. Interface thickness D in lattice units as a function of $(e_c - e)^{-1/2}$.

We also analyzed the surface profiles depicted in Figure 1 in terms of an analytical equation previously derived for the shape of a polymer/polymer interface:[7]

$$\phi(z) = \phi(\infty)[1 - \tanh(2(z-d)/D)]/2 \qquad (7)$$

where D is the full width of the interface (instead of the half-width usually used), d is the location of the interface on the z axis, and $\phi(\infty)$ is the volume fraction in the bulk. The fit of our MC profiles using eq 7 is excellent. The principal parameter from this analysis, the surface thickness D, is plotted in Figure 6 as a function of $(e_c - e)^{-1/2}$. The good fit indicates that the surface thickness can be interpreted by the more familiar formula $D \approx \chi^{-1/2}$ frequently used for the P/P interface. We have not attempted to quantify the surface thickness with relations such as[7] $D = 2b/(6\chi)^{1/2}$, where b is the Kuhn segment length, because the equations of Helfand et al.[7] and Broseta et al.[8] were both appropriate for an interface between polymers, not for a free surface and also for relatively low concentration gradients. In addition, even for an interface between immiscible polymers, Reiter et al.[14] found from MC studies that these MF relations considerably underestimate the interface thickness. To illustrate this point, for our values $e = -0.45$ to -0.7, we calculated D values that range from 0.83 to 0.4 lattice units by using the formula for finite chain lengths of Broseta et al.[8] Similarly, the Sanchez–Poser approach also yields a somewhat narrower interface (see Figure 1).[10]

In contrast, the MC simulations showed that the interfacial thickness D ranges from 2.4 to 5.4 lattice units for reduced cohesion energies between $e = -0.7$ and -0.45. This is thus comparable to the radius of gyration of our chains in the bulk, $R_G = 2.73$ lattice units, and approximately independent of cohesion energy.

Note that the profiles are symmetrical (Figure 1). This result was also observed in the off-lattice MC simulations

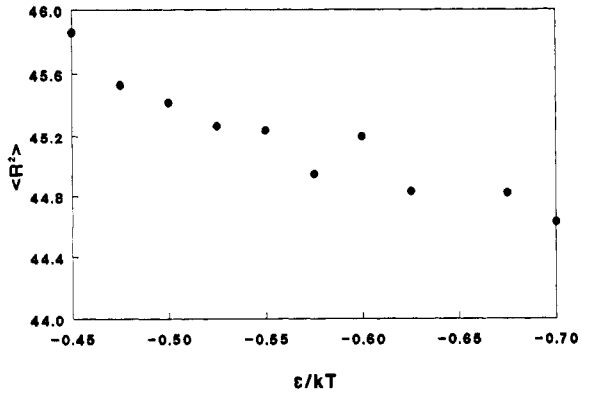

Figure 7. Mean-square end-to-end distance $\langle R^2 \rangle$ in lattice units as a function of reduced cohesive interaction energy in the melt.

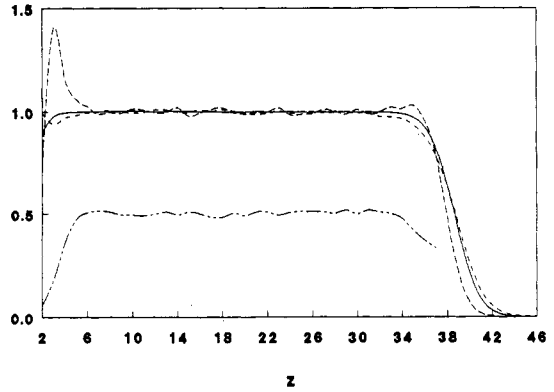

Figure 8. Profiles (normalized to unity in the bulk region) of density (—), chain ends (- - -), coil centers of mass (– –), and coil deformation factor $\langle R_z^2 \rangle / \langle R_x^2 + R_y^2 \rangle$ (– · · –) for $e = -0.5$.

of Mansfield et al.,[2] whereas Poser and Sanchez[10] and Hong and Noolandi[11] predicted asymmetric profiles.

Chain Ends, Centers of Mass, and Segmental Contacts across the Surface. If we consider a condensed polymer melt at various densities, it is well established that, in such a dense entangled medium, chains experience unperturbed chain dimensions. Assuming that the five-choice random walk in a cubic lattice represents an unperturbed chain with average valence angle $\langle \cos \varphi \rangle = -0.2$, we calculated $\langle R^2 \rangle = 45$ lattice units and a Kuhn segment length of $b = 1.5^{1/2}$. Indeed, we found values close to this for the pure polymer melt, although we also observed some deviations (Figure 7). Thus at lower densities, a slight expansion occurred, which could be anticipated from the known concentration dependence of chain dimensions. However, it should be recalled that we consider a condensed system, not a semidilute solution. These changes are not as pronounced as observed[4b] in a polymer mixture with asymmetric compositions and favorable interaction between unlike components. These results point out that, in the pure polymer melt, chain dimensions are not as constant as is often assumed.

Chain-end density is enhanced both at the free surface and at the wall. This can be seen from the profiles (normalized to unity in the bulk region) of chain ends, coil mass centers, and segment densities (Figure 8). However, this enhancement is combined with a depletion layer just below the enriched layer, because the number of chain ends must be conserved within the region of the correlation length given by the dimensions of a single chain. The behavior of chain ends and coil mass centers similar to what is found here for a free surface was also described by Reiter et al.[14] at a P/P interface. The coil-center profile shows layering of coils at the wall and also below the free surface, the effect being stronger at the wall. At the solid

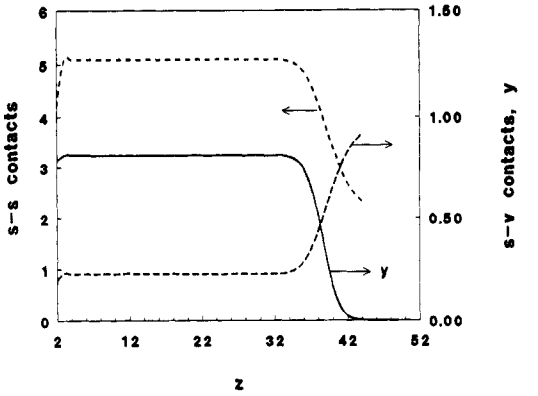

Figure 9. Profile of segment–segment (s–s) and segment–void (s–v) contacts (dashed lines) and the density profile (solid line) across the polymer slab for $e = -0.5$.

wall, the average layer is closer to the wall than the distance R_G (=2.73) because coils are deformed (flattened) in the z direction by the presence of the wall.

Coil deformation both at the wall and at the free surface can be inferred from the behavior of the average $\langle R_z^2 \rangle / \langle R_x^2 + R_y^2 \rangle$, which contains the three components of the end-to-end distance. At both interfaces, flattening in the z direction was observed, whereas in the bulk region this factor attained the unperturbed value of 0.5.

Figure 9 shows the number of contacts of a given chain segment with neighboring segments (s) or voids (v) at a given $e = -0.5$. The total number of nearest neighbors is 6 (except for the $z = 2$ layer, where one contact is with the wall). In the bulk region, the number of s–s contacts is approximately 5, and the number of s–v contacts approximately 1. The number of nonbonded contacts can be obtained effectively by subtracting $(2 - 2/N)$ from the total number of s–s contacts. In the surface region the number of contacts closely parallels the density profile; both the number of s–s and the number of s–v contacts decay or grow at the same rate as the density.

Reduced Surface Tension. By combining the Sanchez–Lacombe EOS theory with the Cahn–Hilliard results for a concentration gradient, Poser and Sanchez[10] (SP) predicted the functional dependence of σ on temperature, pressure, and density. Very good agreement with experimental data was obtained using an adjustment of the free energy gradient coefficient in the overall expression. For comparison, we first repeated the calculation of SP for the chain length of $N = 30$. The resulting surface profiles are also plotted in Figure 1 for $e = -0.45$ and -0.7. Also Figure 3 depicts the results for $\sigma a^2/kT$ according to the SP theory for $N = 30$. From these results, we see that the theoretical approach predicts a somewhat greater density of the melt and produces density profiles somewhat sharper than those obtained from the MC results. As noted earlier, the SP theory also predicts asymmetric profiles rather than the symmetric profiles obtained from the MC simulations.

A number of additional treatments are in principle available for the comparison of the present MC results for surface tension.[15-17] However, we have chosen to restrict the analysis to the SP[10] treatment because of the direct comparison afforded by the latter in terms of real polymers. Thus Helfand's[15] treatment is appropriate to polymer/polymer interfaces with infinite length macromolecules, while the approach of Theodorou describes situations in which there is a sharp density discontinuity at solid walls; in the present contribution we assume a continuous density profile at the interface.

In the following discussion we shall use notation similar to that used in the SP analysis. Thus eq 6 can be expressed

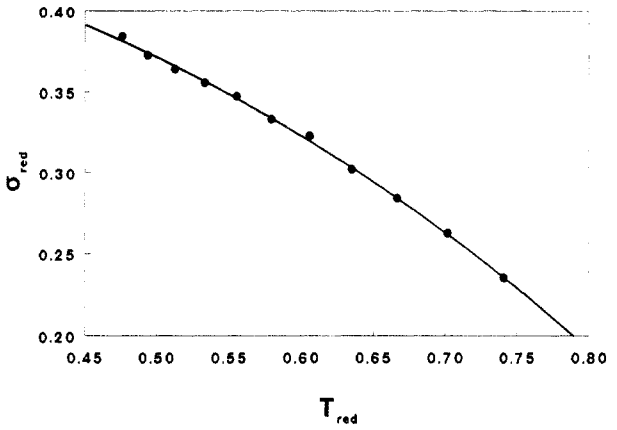

Figure 10. Reduced plot of σ_{red} versus T_{red} calculated for the present MC data according to eq 9.

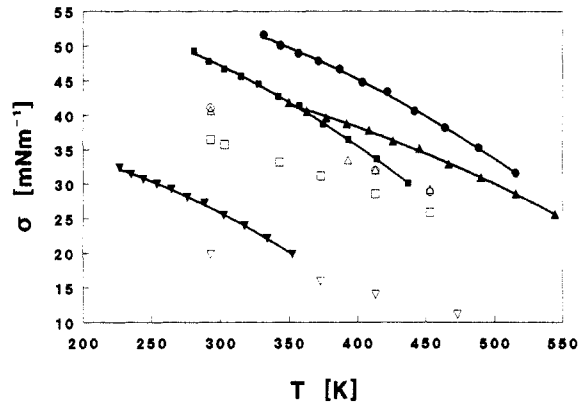

Figure 11. Surface tension as a function of temperature for four polymers obtained from the reduced plot (Figure 10) and bulk EOS parameters ϵ^* and ν^* for PS (▲), PMMA (●), PVAc (■), and PDMS (▼). The experimental results[1,16] are denoted by the corresponding empty symbols.

as a function of a^2 instead of L^2 in the form of reduced units by introducing the EOS parameters: the total interaction energy per segment, ϵ^*, and the close-packed segment volume, ν^*. Thus

$$T^* = \epsilon^*/k, \quad \epsilon^* = |\epsilon|Z/2, \quad T_{red} = T/T^* \tag{8}$$

$$(\nu^*)^{1/3} = a, \quad \sigma^* = \epsilon^*/(\nu^*)^{2/3}, \quad \sigma_{red} = \sigma/\sigma^*$$

After introducing these parameters, we can recast eq 6 as a universal relation between σ_{red} and (implicitly) T_{red}:

$$\sigma_{red} = (4/Z)\langle \sum_i [N_{nb}(z_i,z_i+1) - N_{nb}(z_i,z_i-1)] \rangle \tag{9}$$

It may be noted that this relation is obtained without introducing any approximation for the proportionality factor of the free energy gradient term. However, detailed MC data are needed to evaluate the averaging in eq 9 at a given T_{red}. The plot in Figure 10, based on the present MC results, shows some deviation from the universal plot constructed from the SP theory (see Figures 1 and 7, ref 10), with the present curve located at somewhat higher values of σ_{red}.

In addition to the universal reduced plot (Figure 10), we have calculated (Figure 11) absolute values of σ for polystyrene (PS), poly(methyl methacrylate) (PMMA), poly(vinyl acetate) (PVAc), and poly(dimethylsiloxane) (PDMS) by using appropriate data[18] for ν^* and ϵ^* obtained from the bulk EOS analysis. For comparison, we also show experimental surface tensions.[1,19] The deviations here and in the reduced plot are not surprising, considering the fact that parameters ϵ^* and ν^* have been used here as

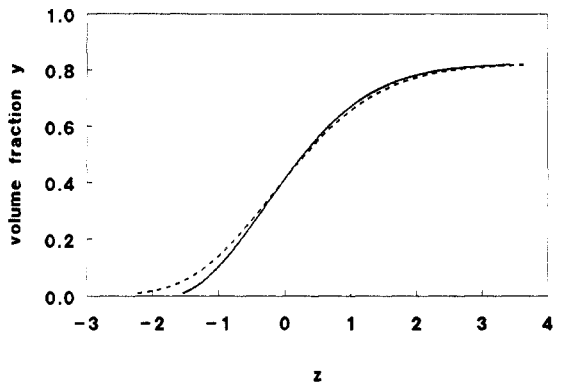

Figure 12. Surface profile from SP theory (solid line) and HN theory (dashed line) for $e = -0.45$ and $N \rightarrow \infty$.

microscopic molecular parameters, whereas they are really phenomenological fitting parameters for a given polymer melt, even when introduced at the molecular level. Furthermore, no fitting of the gradient energy constant to experimental data was performed in the simulation. As an alternative it would be possible to fit the reduced data of eq 9, represented by the plot in Figure 10, to actual σ versus T data for a range of polymers, from which a new set of characteristic parameters ϵ^* and ν^* could be derived. This would possibly produce a satisfactory agreement of experimental data on one universal curve, but has not been pursued for two reasons. First, we wish to present the present *ab initio* analysis independently, and secondly, the present data have been obtained only for $N = 30$ and not for the asymptotic value $N \rightarrow \infty$, for which the expanded results would be more appropriate.

From the experimental value for the parameter ν^* obtained from eq 7, an approximate absolute value for an effective lattice spacing unit for surface profiles and hence the surface thickness can be obtained. For polystyrene we found[20] $a = 0.55$ nm, and we have thus calculated that the surface thicknesses of the profiles shown in Figure 1 are approximately $D \approx 1.5$–4.0 nm.

It is noted that Hong and Noolandi[11] (HN) have developed a polymer surface tension theory based on a functional integral theory approach by accounting for conformational entropy effects not present in the SP theory. The HN approach yields surface tensions higher than those derived by SP theory (see Figure 3). The interface profiles calculated for $N \rightarrow \infty$ and $e = -0.45$ (Figure 12) are very similar. The HN profile is somewhat wider than the SP profile, with differences mainly on the low-density side of the profile. As can be seen, both profiles are asymmetric. We can conclude that the HN theory, predicting somewhat higher σ values and a slightly thicker interface than those of the SP theory, is somewhat closer to our results (compare Figures 1, 3, 10, and 12).

Despite the limitation imposed by the lattice approximation used here, we believe the present simulation results provide a reasonably accurate estimate of the surface parameters of a polymer melt. Our contention is based on the good agreement of the calculated surface tension and its temperature coefficient and the fact that the symmetric surface profiles are supported by the off-lattice simulation of Mansfield et al.[2] Finally, a parallel simulation of the surface segregation of a polymer blend near a solid wall produced excellent agreement with mean-field theory, again without using additional fitting parameters.[21]

Acknowledgment. We gratefully acknowledge the support of the Air Force Office of Scientific Research through Grant No. 93-001.

References and Notes

(1) Wu, S. *Polymer Interface and Adhesion*; Marcel Dekker: Basel, 1982.
(2) Mansfield, K. F.; Theodorou, D. N. In *Computer Simulation of Polymers*; Roe, R. J., Ed.; Prentice-Hall: Englewood Cliffs, NJ, 1991; p 122.
(3) (a) Madden, W. G. *J. Chem. Phys.* **1987**, *87*, 1405. (b) Madden, W. G.; Pesci, A. I.; Freed, K. F. *Macromolecules* **1990**, *23*, 1181.
(4) (a) Cifra, P.; Karasz, F. E.; MacKnight, W. J. *Macromolecules* **1992**, *25*, 4895. (b) Cifra, P.; Karasz, F. E.; MacKnight, W. J. *Macromolecules* **1992**, *25*, 192.
(5) Boyd, R. H. *Macromolecules* **1989**, *22*, 2477.
(6) Dickman, R.; Hall, C. K. *J. Chem. Phys.* **1988**, *89*, 3168.
(7) (a) Helfand, E.; Tagami, Y. *J. Chem. Phys.* **1971**, *56*, 3592. (b) Helfand, E.; Tagami, Y. *Ibid.* **1972**, *57*, 1812.
(8) Broseta, D.; Fredrickson, G.; Helfand, E.; Leibler, L. *Macromolecules* **1990**, *23*, 132.
(9) Binder, K. *J. Chem. Phys.* **1983**, *79*, 6387.
(10) Poser, C. I.; Sanchez, I. C. *J. Colloid Interface Sci.* **1979**, *69*, 539.
(11) Hong, K. M.; Noolandi, J. *Macromolecules* **1981**, *14*, 1229.
(12) Rowlinson, J. S.; Widom, B. *Molecular Theory of Capillarity*; Clarendon Press: Oxford, 1989.
(13) Nies, E.; Cifra, P., submitted to *Macromolecules*.
(14) Reiter, J.; Zifferer, G.; Olaj, O. F. *Macromolecules* **1990**, *23*, 224.
(15) Helfand, E. *J. Chem. Phys.* **1975**, *63*, 2192.
(16) Theodorou, D. N. *Macromolecules* **1988**, *21*, 1391, 1911, 1922.
(17) Szleifer, I.; Widom, B. *J. Chem. Phys.* **1989**, *90*, 7529.
(18) Sanchez, I. C. In *Encyclopedia of Physical Science and Technology*; Academic Press: New York, 1992; Vol. 13.
(19) Sanchez, I. C. *Polym. Eng. Sci.* **1984**, *24*, 79.
(20) Nies, E.; Stroeks, A. *Macromolecules* **1990**, *23*, 4088.
(21) Cifra, P.; Bruder, F.; Brenn, R. *J. Chem. Phys.* **1993**, *99*, 4121.